Could a slow stable hybrid star explain the central compact object in HESS J1731-347?

Mauro Mariani,[1,2,*] Ignacio F. Ranea-Sandoval,[1,2,†] Germán Lugones,[3,‡] and Milva G. Orsaria[1,2,§]

[1]*Grupo de Astrofísica de Remanentes Compactos, Facultad de Ciencias Astronómicas y Geofísicas, Universidad Nacional de La Plata, Paseo del Bosque S/N, La Plata (1900), Argentina*

[2]*CONICET, Godoy Cruz 2290, Buenos Aires (1425), Argentina*

[3]*Universidade Federal do ABC, Centro de Ciências Naturais e Humanas, Avenida dos Estados 5001- Bangú, CEP 09210-580, Santo André, São Paulo, Brazil*

(Received 31 May 2024; accepted 16 July 2024; published 19 August 2024)

We explore an alternative explanation for the low-mass ultracompact star in the supernova remnant HESS J1731-347 using a model-agnostic approach to construct hybrid equations of state. The hadronic part of the hybrid equation of state is constructed using a generalized piecewise polytropic scheme, while the quark phase is described by the generic constant speed of sound model. We assume an abrupt first-order hadron-quark phase transition with a slow conversion speed between phases. Our equations of state align with modern chiral effective field theory calculations near nuclear saturation density and are consistent with perturbative quantum chromodynamics calculations at high densities. Using this theoretical framework, we derive a wide range of hybrid equations of state capable of explaining the light compact object in HESS J1731-347 in a model-independent manner, without fine-tuning. These equations of state are also consistent with modern astronomical constraints from high-mass pulsar timing, NICER observations, and multimessenger astronomy involving gravitational waves. Our results support the hypothesis that the compact object in HESS J1731-347 could plausibly be a slow stable hybrid star.

DOI: 10.1103/PhysRevD.110.043026

I. INTRODUCTION

The lightest neutron star (NS) confirmed to date, with a mass of $M = 1.174 \pm 0.004 M_\odot$, is located within a double pulsar system known as J0453 + 1559 [1,2] (although the authors of Ref. [3] propose that the lower-mass component of J0453 + 1559 might be a white dwarf instead of a NS). However, the recent discovery of a potentially even lighter NSs poses a new challenge to astrophysics in the quest for understanding the equation of state (EOS) for dense matter. In a recent paper, Doroshenko *et al.* [4] estimated, after modeling the x-ray spectrum and using a Gaia-observation-based distance, the mass, M, and radius, R, of the central compact object (CCO) in the supernova remnant HESS J1731-347. The best values obtained for these quantities are $M = 0.77^{+0.20}_{-0.17} M_\odot$ and $R = 10.4^{+0.86}_{-0.78}$ km, respectively, at the 1σ posterior credible levels.

It is important to recall, however, that several assumptions are needed to obtain such tight results. In particular, it is assumed that the atmosphere of the NS is predominantly composed of carbon and that it has a uniform temperature distribution; such hypothesis, leading to a strong model dependence, is subject to criticism and discussion. Indeed, recent studies claim that most known CCOs do not exhibit uniform-temperature carbon atmospheres [5]. Instead, they would show evidence of nonuniform temperature surfaces with small hot spots, suggesting that uniform-temperature carbon atmospheres might not be a common characteristic among observed CCOs, and instead, multitemperature surfaces are more typical. In fact, the analysis made by Alford and Halpern [5] of the longest, highest-quality dataset from XMM-Newton produces results inconsistent with a uniform-temperature carbon atmosphere model, as suggested by Doroshenko *et al.* [4], whether or not attempts are made to model dust scattering. Doroshenko *et al.* [4] also considered other viable assumptions and the results obtained for the mass and radius of the CCOs are different. Reference [5] also highlights another key aspect; the assumption made by Doroshenko *et al.* [4] regarding the distance at which the CCO is located is crucial. Their use of a distance estimate of 2.5 kpc, not supported by other studies, is critical for concluding that the mass of the CCO in HESS J1731-347 is significantly lower than that of a canonical NS. It is also important to note that such estimation is in tension with numerical simulations of supernovae explosions, which suggest that the minimum possible mass for the remnant NS has to be larger (see, for

*Contact author: mmariani@fcaglp.unlp.edu.ar
†Contact author: iranea@fcaglp.unlp.edu.ar
‡Contact author: german.lugones@ufabc.edu.br
§Contact author: morsaria@fcaglp.unlp.edu.ar

example, Ref. [6] and references therein). Nevertheless, if these values are confirmed by future observations and more detailed analysis, such object would be one of the least massive and smallest compact objects ever observed. Hence, it represents a relevant and challenging observation to analyze and elucidate.

In addition to these low-mass compact objects, there are other astronomically relevant estimations of mass and radius from double pulsars [7–11], multimessenger astronomy with gravitational waves from event GW170817 [12–15] and NICER observations of the isolated NS PSR J0030 + 0451 [16,17] and the double pulsar PSR J0740 + 6620 [18,19]. Current dense matter EOS and compact object models should simultaneously address all these astrophysical constraints, along with those from nuclear and particle data. Regarding this latter family of restrictions, there are constraints for the dense matter EOS in the two limit regimes of low and high density. For densities $n \lesssim n_0$, with $n_0 = 0.16\ \mathrm{fm}^{-3}$ the nuclear saturation density, the EOS is determined with accuracy due to nuclear theory and experiments. For the range $n_0 \lesssim n \lesssim 2n_0$, there are calculations based on the chiral effective field theory (cEFT). Recently, various improved cEFT calculations have been published [20–24]; in our work, we use the calculations provided by Drischler *et al.* [25], who obtained a refined constraint for β-stable NS matter up to $2n_0$ using a Bayesian framework for quantifying and propagating correlated cEFT truncation errors. For very high densities, in the $n \gtrsim 40n_0$ regime, perturbative QCD (pQCD) calculations help understand the behavior of deconfined matter and derive the corresponding EOS [26]. As we will discuss later, such extreme densities, although unusual or absent in traditional hadronic NSs, could be relevant in some exotic scenarios [27].

According to the proposals in the literature, NSs constructed with soft EOSs can explain the low-mass object observed in HESS J1731-347 (see, for example, Refs. [28,29] and references therein for modern studies on this scenario). In addition to these models, other exotic theoretical scenarios have been proposed to explain such a low-mass compact object. In Refs. [28,30], the authors analyzed the possibility that this compact object might be a hybrid star (HS). Furthermore, more radical theoretical possibilities have been explored; for example, it has been proposed that the HESS J1731-347 object might be a strange quark star (SQS) (see, for example, Refs. [28,31–35] and references therein) or a compact object in which normal matter is admixed with dark matter [28].

In view of the wide variety of theoretical alternatives proposed in the literature regarding the nature of the compact object at the center of the HESS J1731-347 supernova remnant, we aim to explore the possibility that the low-mass compact object could be a *slow stable* hybrid star (SSHS), a concept previously introduced and discussed in several papers [27,36–47]. SSHSs are compact stars with a sharp hadron-quark phase transition that could remain stable even though $\partial M/\partial \epsilon_c < 0$, when considering a *slow* hadron-quark conversion speed such that the conversion timescale is larger than the typical oscillation timescale. Within this theoretical possibility, perturbed fluid elements at the phase-transition surface do not have enough time to convert quarks into hadrons (or vice versa). For this reason, motion around the interface solely involves stretching and compression of volume elements but with no transformation between the different phases. This feature differentiates these configurations from the more traditional totally stable hybrid stars (TSHSs), which are located in branches that satisfy $\partial M/\partial \epsilon_c > 0$ and are stable under both *slow* and *rapid* conversion scenarios. The significance of SSHSs lies in their potential to explore extreme regions of the QCD phase diagram through astronomical observations of compact objects. Moreover, as stated in Ref. [27], ultrastiff EOSs should not be discarded, as astronomical constraints (such as those from GW170817 and its electromagnetic counterpart, along with the radius measurement of PSR J0740 + 6620) can be satisfied by SSHSs.

The paper is organized as follows. In Sec. II we describe the parametric model used to construct the hybrid EOS and the role of sharp and slow hadron-quark phase transitions in the stability analysis of HSs. Section III presents the most important results of our study, while their astronomical implications are discussed in Sec. IV.

II. HYBRID EOS CONSTRUCTION CRITERIA

In this section, we outline the criteria used for constructing the hadron and quark EOSs, as well as the phase transition associated with the hybrid EOS. To make our study of HSs comprehensive and independent of specific hadron and quark EOSs models, we consider generic parametric forms of the hybrid EOSs. These forms allow us to fit not only the constraints imposed by cEFT but also those arising from pQCD, representing a diverse range of microscopic hybrid EOSs.

To construct the hadron sector of the hybrid EOS, we follow the prescription of Ref. [48], as previously done in Refs. [27,42–44], and consider the Baym Pethick Sutherland (BPS)-Baym Bethe Pethick (BBP) crust [49,50]. We use the BPS-BBP crust up to $0.5n_0$, and beyond this density, we apply the Generalized Piecewise Polytropes (GPP) prescription, ensuring continuity in n, P, and ϵ at the juncture. The junction density $0.5n_0$ corresponds to the value $\log_{10}(\rho_0) = 14.127$, marking the beginning of the first section of the piecewise polytropic EOS.

In this way, we have constructed three representative hadronic EOSs, labeled as soft, intermediate, and stiff. The detailed parameters of each hadron EOS are presented in Table I. The choice of the limiting soft and stiff EOSs allow us to span a wide range of hadronic EOSs consistent with cEFT. The inclusion of an intermediate EOS aims to enrich our study and broaden its scope. In Fig. 1(a), we show their $P - \epsilon$ relationship along with current constraints from cEFT [25] and pQCD [26,51,52]; in the right panel, we

TABLE I. Parameters of the selected hadronic EOSs constructed using the prescription of Ref. [48] and the BPS-BBP crust [49,50] up to $0.5n_0$. In all cases, we adopted $\log_{10}(\rho_0) = 14.127$ and $\log_{10}(K_1) = -27.22$ because the crust ends at $0.5n_0$. The EOSs are also consistent with the boundaries of the region allowed by cEFT presented in Ref. [25], as shown in Fig. 1(a).

	$\log_{10}\rho_1$	$\log_{10}\rho_2$	Γ_1	Γ_2	Γ_3
Soft	14.30	14.65	2.757	3.4	2.70
Intermediate	14.50	14.65	2.763	5.1	2.35
Stiff	14.55	14.65	2.766	9.5	1.05

show the correspondent $M-R$ relationships along with current astrophysical constraints. It can be observed how soft and stiff EOSs act as enveloping curves for this low-density cEFT constraint (considered up to $1.5n_0$, as model uncertainties tend to increase for larger densities); the intermediate EOS is in between of them, in both the $P-\epsilon$ and M-R planes. Moreover, by construction, the soft hadronic EOS satisfies all current astronomical constraints by its own (in agreement with some previous works mentioned in Sec. I; the intermediate one satisfies all current astronomical constraints except the one associated with HESS J1731-347; the stiff one satisfies all current astronomical constraints except those from HESS J1731-347 and GW170817. Additionally, the stiff EOS does not satisfy the $M_{\rm max} \lesssim 2.3M_\odot$ condition either [53–55]. However, in the HS Tolman-Oppenheimer-Volkoff (TOV) integration, the appearance of the quark core will allow it to satisfy the maximum mass upper constraint. In this sense, soft and stiff EOSs act as limiting extreme cases also in the M-R plane, representing the frontier zone of the minimum and maximum allowed radius and masses, respectively.

For the quark sector, we consider the constant speed of sound (CSS) model [57]. This model is a general parameterization used to represent qualitative aspects of various models of quark matter, suitable for high-density EOS and characterized by a first-order abrupt hadron-quark phase transition, where the speed of sound in the quark phase is independent of pressure. The model consists of three parameters; the hadron-quark transition pressure, P_t, the size of the energy density transition jump, $\Delta\epsilon$, and the squared speed of sound of the quark phase, c_s^2, which is constant within the model.

Both the parametric models for hadron and quark matter enable us to extensively explore the hybrid EOS space, aiming to obtain general qualitative and model-independent results. Thus, considering an abrupt first-order hadron-quark transition, we have constructed

$$3(\text{hadron}) \times 13(P_t) \times 13(\Delta\epsilon) \times 3(c_s^2) = 1521$$

hybrid EOSs using the three soft, intermediate, and stiff hadronic EOSs, and the following parameter ranges for the CSS quark EOS:

$$10\ \text{MeV/fm}^3 \le P_t \le 300\ \text{MeV/fm}^3,$$
$$100\ \text{MeV/fm}^3 \le \Delta\epsilon \le 3000\ \text{MeV/fm}^3,$$
$$c_s^2 = 0.33, 0.50, 0.70.$$

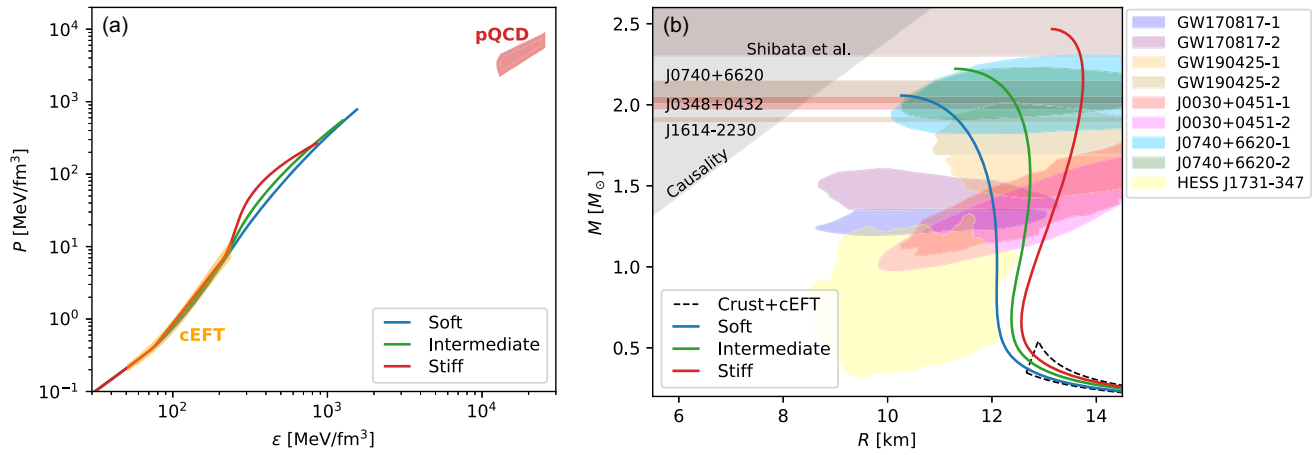

FIG. 1. P-ϵ and M-R relationship for the soft, intermediate, and stiff hadronic EOSs. (a) In the P-ϵ plane, the EOSs are presented up to the energy density value reached at the center of the maximum mass NS configuration. Constraints are provided by cEFT and pQCD as presented in Ref. [25] and Ref. [52], respectively. (b) In the M-R plane we also show astrophysical constraints from the $\sim 2M_\odot$ pulsars [7–11], GW170817 [13,14] and GW190425 [56] events (90% posterior credible level), NICER pulsars (2σ posterior credible level) [16–19], and HESS J1731-347 (2σ posterior credible level) [4]. The upper-horizontal area is the region excluded by Shibata *et al.* [53], $M_{\rm max} \le 2.3M_\odot$. The shaded region in the upper-left corner indicates the causality forbidden zone. The dashed black curve shows the TOV integrated region of the cEFT constraint. These hadronic EOSs represent extreme limiting cases for both nuclear and astrophysical constraints (see text for details).

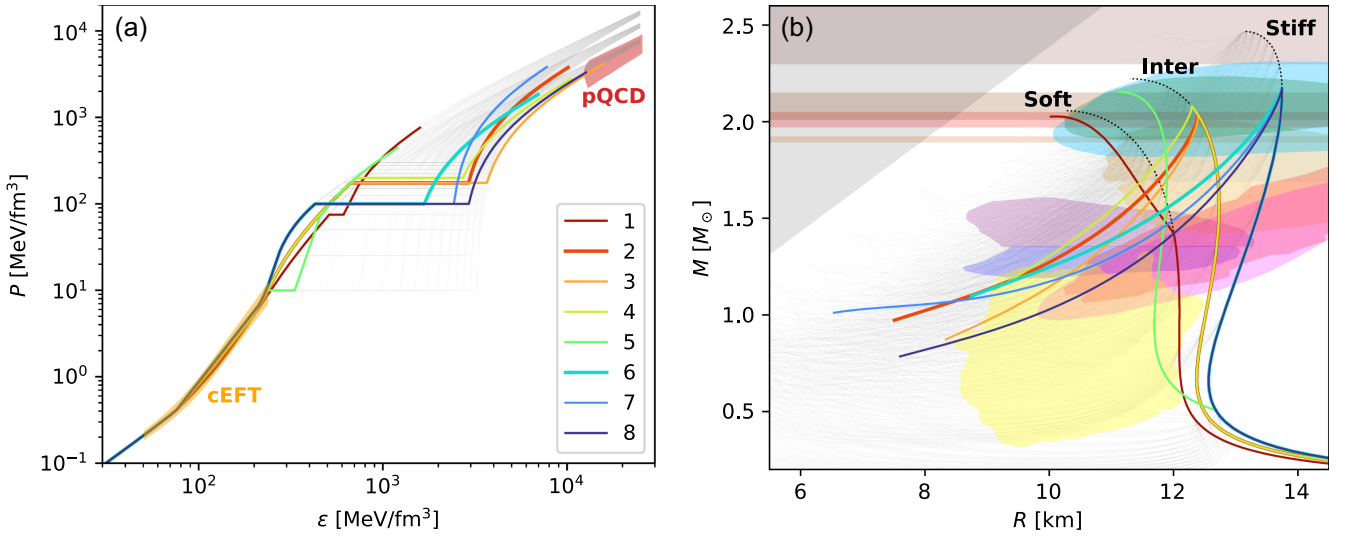

FIG. 2. (a) The eight selected hybrid EOSs are shown in color, along with the cEFT constraint up to $1.5n_0$ [25] and pQCD results for $n \gtrsim 40n_0$ [26,51,52]. The selected EOSs are displayed up to the largest central density reached in each HS model. Details of the EOSs are provided in Table II. All 1521 constructed hybrid EOSs, up to the largest calculated density, are shown in light gray. (b) Mass-radius relationships for the EOSs in the panel (a); the same color-coding is used for the eight selected cases. The fully hadronic soft, intermediate, and stiff curves are shown in black as a reference. Since SSHSs are considered, all curves are shown up to the terminal configuration, and thus all points of the curves represent dynamically stable stars. The colored shaded regions represent the constraints described in Fig. 1. The TOV results for all 1521 hybrid EOSs are presented in light gray.

All of the 1521 constructed EOSs satisfy the cEFT constraint. Only the EOS with $c_s^2 = 0.33$ fulfill the pQCD constraint, while the EOSs with $c_s^2 = 0.50, 0.70$ do not [see light gray curves in Fig. 2(a)]. However, we do not discard them yet, as they remain valid if the central density and pressure of the last stable NS configuration do not exceed the pQCD densities and pressures, as we will discuss later.

It is crucial to mention at this point that the speed of the conversion between hadronic and quark matter at the phase transition surface plays a key role in the stability analysis of HSs [36] (see also [58] for a review on the subject). First-order phase transitions are highly collective nonlinear phenomena and, for this reason, the conversion timescale between phases might not conform to the typical interaction timescales. Nucleation is one of the preferred mechanisms to model such processes (see, for example, Ref. [59] and references therein). It is important to recall that alternative theoretical approaches are available in the literature (see, for example, Refs. [60,61] and references therein). Within the nucleation scenario, a direct conversion between hadronic and quark phases in β equilibrium is suppressed as the phases have, in principle, very different flavor compositions. For this reason a two-step conversion mechanism has been proposed [59,62,63]. This establishes the slow conversion regime (where conversion timescales may exceed a few milliseconds) as a plausible scenario for a mechanism not yet fully understood (for a more detailed discussion, see the recent review [58] and references therein). In this scenario, a (long) branch of SSHSs with $\partial M/\partial \epsilon_c < 0$ can be present after solving the TOV equations that determine stationary stellar configurations [37–41,45,47,64,65]. For this reason, to construct the abrupt phase-transition, we work within the *slow* hadron-quark conversion scenario, which gives rise to SSHSs configurations located on an extended stability branch following the maximum mass configuration in the M-R relationship. This contrasts with the traditional TSHSs that are stable in both the *rapid* and *slow* scenarios along the $\partial M/\partial \epsilon_c > 0$ branches.

III. RESULTS

Given the extensive sampling of hybrid EOSs constructed in the previous section, we select eight of them that satisfy all current nuclear and astrophysical constraints, including HESS J1731-347. In Table II we present the details of these EOSs, which exhibit different hadronic components and a wide range of the CSS parameters. We selected them to demonstrate the variety in qualitative EOS behaviors and the lack of need of fine tuning. It is important to note that the selected EOSs serve as representatives of EOS families with common qualitative morphology that satisfy the constraints, as numerous sampled EOSs meet these criteria beyond the particular eight selected. Additionally, we aimed to include EOSs that are potentially limiting or extreme cases, to serve as enveloping samples for intermediate cases (see the discussion below regarding EOSs 2 and 7).

In Fig. 2(a), we present the results for the selected hybrid EOSs, along with all 1521 hybrid EOSs constructed, show

TABLE II. Parameters of the eight selected EOSs among the 1521 constructed hybrid EOSs (see text for more details).

No.	Hadronic	$P_t(\mathrm{MeV/fm^3})$	$\Delta\epsilon(\mathrm{MeV/fm^3})$	c_s^2
1	Soft	75	100	0.70
2	Intermediate	175	2250	0.50
3	Intermediate	175	3000	0.33
4	Intermediate	200	2000	0.33
5	Stiff	10	100	0.50
6	Stiff	100	1250	0.33
7	Stiff	100	2000	0.70
8	Stiff	100	2500	0.33

as light gray curves in the background. In addition to the $P-\epsilon$ relationships, we include the cEFT and pQCD constraints. The EOS curves depict the hadron phase for lower densities up to the abrupt phase transition indicated by the energy density jump, and the quark sector for higher densities. These EOSs are presented up to the maximum energy density reached in the stable NS core. As shown, for the cases with $c_s^2 = 0.50,\ 0.70$, the physically relevant energy density and pressure ranges do not exceed—and are thus compatible with—the pQCD prediction. In particular, EOSs 2 and 7 present a limiting case in terms of pQCD compatibility; we select these two to sample these extreme yet possible cases where a sequential second phase transition could occur in the extreme high-density regime. The other selected EOSs automatically satisfy pQCD as they have $c_s^2 = 0.33$ (EOSs 3, 4, 6 and 8) or they do not reach such high densities in the NS cores and could potentially exhibit a smooth decrease in the speed of sound (EOSs 1 and 5). The numerous gray curves show that, for large densities, the EOSs converge into three distinctive families corresponding to $c_s^2 = 0.33, 0.50, 0.70$, and that only $c_s^2 = 0.33$ satisfies pQCD for these densities.

In Fig. 2(b) we show the $M-R$ relationships for the selected EOSs. Similar to Fig. 2(a), we include all 1521 TOV results as light gray curves in the background. Each configuration shown in the figure is dynamically stable within the slow conversion regime (i.e., after solving the radial perturbation equations, we find that their fundamental radial eigenfrequency is real until the *terminal mass*, at which point it vanishes). We can see that every astronomical constraint is satisfied by these representative cases. EOSs 1 and 5, with the lowest transition pressures, become hybrid for relatively low masses, exhibit short extended branches, and satisfy the constraints with their TSHS branches. EOS 1 corresponds to a soft hadronic EOS (satisfying the constraints without any hadron-quark transition); a high speed of sound in the quark sector, $c_s^2 = 0.70$, allows the hybrid branch to extend beyond $2.01M_\odot$, satisfying all constraints even with the occurrence of the hadron-quark phase transition. For this EOS, the HESS J1731-347 object would be a hadronic NS, while GW170817 objects could be both hadronic and/or hybrid configurations. On the other hand, EOS 5 corresponds to a stiff hadronic EOS, and the very early phase transition, along with decreasing radii, enables it to satisfy HESS J1731-347 and GW170817 constraints through a TSHS branch with very low masses. As already shown in Lugones *et al.* [27], these two EOSs confirm that the low-pressure transition scenario remains valid for meeting modern astrophysical constraints. However, the kind of compact objects produced by these two EOSs are well-studied [28–30], do not involve the SSHS branch, and are not the primary focus of our work. The remaining six EOSs are selected to show that the extended SSHS branch is a possible alternative model for simultaneously meeting the HESS J1731-347 and PSR 0740 + 6620 constraints. These six EOSs produce a stable hadronic branch with large radii up to a maximum mass configuration. At this point, the hadron-quark phase transition occurs, followed by a steep and extended SSHS branch that overlaps with the HESS J1731-347 measurement, roughly at $1M_\odot$ and within the 9–11 km range.

Although the soft EOS is not the optimal candidate for producing SSHSs that satisfy current constraints due to its low maximum mass and small radii, both the intermediate and the stiff EOSs offer an extended parameter space that meets all requirements. Our results suggest that the CCO in HESS J1731-347 could be either a purely hadronic NSs or a SSHSs. In particular, they indicate that the HESS J1731-347 object could be a particularly compact and low mass SSHS, provided the hadronic EOSs lies between the intermediate and stiff cases. As our generic proposals are constructed to be model-independent limiting cases, numerous microphysical EOS models in the literature likely fall within these bounds and could inherit the implications of our findings.

In Fig. 3(a) we present our results for the dimensionless tidal deformability, Λ, in the Λ-M plane, along with the constraint arising from the GW170817 event for a $1.4M_\odot$ configuration [14]. Similar to the M-R results, EOSs 1 and 5 satisfy this constraint through the totally stable branch, purely hadronic for EOS 1 and hybrid for EOS 5. The other EOSs with long SSHS branches satisfy this constraint through the extended stability branch, which exhibits a nonmonotonic behavior of Λ as a function of M, with the $1.4M_\odot$ configuration being a SSHS. In Fig. 3(b), we show the individual dimensionless tidal deformabilities in the Λ_1-Λ_2 plane, considering the stellar configuration pairs that match the chirp mass of the GW170817 binary neutron star merger and the 50% and 90% confidence contours for this event (both assuming low-spin priors) [14,15,66]. In this figure, there are numerous disconnected branches for each EOS as different types of compact object combinations are considered. The region where $\Lambda_1 > \Lambda_2$ is populated since in the *slow* conversion stability scenario, Λ can increase with M. Every EOS has at least one branch combination that falls inside the confidence regions. Combinations

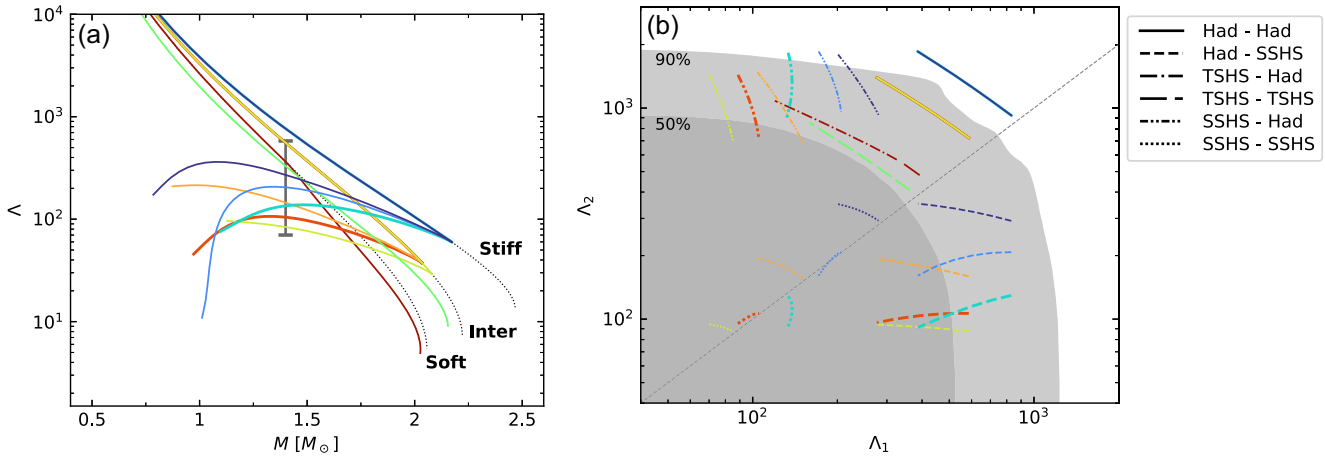

FIG. 3. (a) Dimensionless tidal deformability, Λ, as a function of the gravitational mass, M, for the EOSs of Fig. 2 (same colors are used). Since we are considering slow hadron-quark conversions and SSHSs extended branches, all the shown curves represent dynamically stable configurations. The fully hadronic soft, intermediate, and stiff curves are shown in black as a reference. The gray vertical segment represents the constraint imposed for a $1.4M_\odot$ NS by the analysis of the GW170817 event [14]. (b) Individual tidal deformabilities Λ_1, Λ_2 for binary neutron star mergers with the same chirp mass as the GW170817 binary system [14,15,66] for the EOSs of Fig. 2 (same colors are used). Each line type indicates the kind of objects potentially involved in the binary merger. For slow conversions, $\Lambda_1 > \Lambda_2$ is possible because Λ does not necessarily decrease with M. Dark and light gray areas represent the 50% and 90% confidence levels of the GW170817 event, respectively.

including SSHS-type objects are statistically preferred as they mostly fall inside the 50% region, compared to purely hadronic and/or TSHS pairs.

IV. SUMMARY AND DISCUSSION

In this work, we provided an alternative explanation for the CCO in the supernova remnant HESS J1731-347. For the first time, we showed that SSHSs are viable candidates to explain the observed mass and radius of this ultracompact star using a model-agnostic approach to construct hybrid EOSs.

We constructed 1521 hybrid EOSs satisfying the cEFT constraint using parametric EOSs suitable for the crust-hadron and quark phases; the generic BPS-BBP-GPP and CSS models, respectively. Eight of them were selected to represent a variety of EOSs with qualitative different behaviors without requiring fine-tuning, while still satisfying all current nuclear and astrophysical constraints, including those from HESS J1731-347. In selecting the EOSs, we also took into account results from pQCD calculations. This constraint is fulfilled by EOSs 3, 4, 6, and 8 by construction ($c_s^2 = 0.33$); by EOSs 2 and 7 if there is a second abrupt phase transition at very high density; and by EOSs 1 and 5 if a smooth decrease in the speed of sound is assumed beyond the largest NS density. Our results show that the characteristics of the HESS J1731-347 object can be explained by some models of pure hadronic stars and traditional hybrid stars. However, this is only possible for very specific hadronic models (soft hadronic EOS) or traditional hybrid models with a phase transition at very low density (EOSs 1 and 5). In contrast, our results demonstrate that there is a wide variety of SSHS models that naturally satisfy the HESS J1731-347 observation.

Regarding the dimensionless tidal deformability Λ and the $\Lambda_1 - \Lambda_2$ relationship, the obtained results are similar to those of Ref. [27]; in the context of SSHSs, the most massive component of a binary compact object merger would not necessarily have the smallest Λ. Additionally, in line with the findings of the aforementioned work, binary systems involving at least one object from the SSHS branch rather than only combinations of the traditional hadronic and/or TSHS ones, could be considered as an alternative explanation for the GW170817 event.

Our model for HESS J1731-347 avoids some potential issues that other theoretical proposals might encounter. For instance, the ultrasoft hadronic EOS needed to provide a (nonmarginal) explanation for HESS J1731-347 as a purely hadronic NS are in tension with modern results from cEFT calculations. As discussed and summarized in Refs. [67–69], various modern cEFT calculations for the low-density region of the hadronic EOS exist (e.g., Refs. [20–24]); in this study, as previously mentioned, we applied the constraints presented in Drischler *et al.* [25]. However, any of the more recent cEFT constraints strongly restrict the low-density EOS regime, requiring even more careful tuning of the hadronic model to match the results of HESS J1731-347.

On the other hand, concerns have been raised about the idea that HESS J1731-347 might be a SQS, mainly because observations indicate that the star's surface temperature is quite high [4]. This would conflict with the rapid cooling expected in quark matter due to the onset of the quark direct

URCA process (see, for example, Refs. [70–72] and references therein). However, a viable explanation for the surface temperature of HESS J1731-347 could be achieved if quarks form color superconducting pairs with a small gap, which suppresses the fast cooling [28,32]. The primary obstacle of this interpretation lies in the inherently speculative nature of the strange quark matter hypothesis, which requires not only the formation of deconfined quark matter in compact objects but also that such matter be self-bound.

On the other hand, models suggesting that the HESS J1731-347 object comprises normal matter admixed with dark matter require a dark matter fraction of approximately 5% of the total NS mass to account for the observed mass and radius of this object (see, e.g., Ref. [28] and references therein). Considering that the local dark matter mass density in the solar neighborhood is estimated to be around $0.01 M_{\odot}\ \mathrm{pc}^{-3}$ [73], the capture efficiency of dark matter particles appears exceedingly low [74], making it difficult to justify how such a significant amount of dark matter could accumulate inside the compact object in HESS J1731-347, which is only a few kyr old.

To conclude, both the precise characteristics of the HESS J1731-347 compact object and the existence of SSHSs (given the ongoing debate surrounding the nature of the hadron-quark phase transition) remain open questions. If SSHS are indeed possible, and if future observations were to confirm the lowest mass NS to date within HESS J1731-347, SSSHs could provide a plausible explanation for this compact object and shed light on the still unknown EOS of NSs.

ACKNOWLEDGMENTS

M. M. thanks C. Drischler for providing the data constraints for cEFT. M. M, I. F. R-S., and M. G. O acknowledge UNLP and CONICET for financial support under Grants No. G187 and No. PIP-0169. M. M is a postdoctoral fellow of CONICET. I. F. R-S. is also partially supported by PIBAA 0724 from CONICET. I. F. R-S. and M. G. O. are partially supported by the National Science Foundation (USA) under Grant No. PHY-2012152. G. L. acknowledges the financial support from CNPq (Brazil) Grant No. 316844/2021-7 and FAPESP (Brazil) Grant No. 2022/02341-9.

[1] J. Martinez, K. Stovall, P. Freire, J. Deneva, F. Jenet, M. McLaughlin, M. Bagchi, S. Bates, and A. Ridolfi, Pulsar j0453 + 1559: A double neutron star system with a large mass asymmetry, Astrophys. J. **812**, 143 (2015).
[2] F. Özel and P. Freire, Masses, radii, and the equation of state of neutron stars, Annu. Rev. Astron. Astrophys. **54**, 401 (2016).
[3] T. M. Tauris and H.-T. Janka, J0453 + 1559: A neutron star–white dwarf binary from a thermonuclear electron-capture supernova?, Astrophys. J. Lett. **886**, L20 (2019).
[4] V. Doroshenko, V. Suleimanov, G. Pühlhofer, and A. Santangelo, A strangely light neutron star within a supernova remnant, Nat. Astron. **6**, 1444 (2022).
[5] J. A. J. Alford and J. P. Halpern, Do central compact objects have carbon atmospheres?, Astrophys. J. **944**, 36 (2023).
[6] Y. Suwa, T. Yoshida, M. Shibata, H. Umeda, and K. Takahashi, On the minimum mass of neutron stars, Mon. Not. R. Astron. Soc. **481**, 3305 (2018).
[7] P. Demorest, T. Pennucci, S. Ransom, M. Roberts, and J. Hessels, Shapiro delay measurement of a two solar mass neutron star, Nature (London) **467**, 1081 (2010).
[8] J. Antoniadis *et al.*, A massive pulsar in a compact relativistic binary, Science **340**, 448 (2013).
[9] Z. Arzoumanian *et al.*, The NANOGrav 11-year data set: High-precision timing of 45 millisecond pulsars, Astrophys. J. Suppl. Ser. **235**, 37 (2018).
[10] H. T. Cromartie *et al.*, Relativistic Shapiro delay measurements of an extremely massive millisecond pulsar, Nat. Astron. **4**, 72 (2020).
[11] E. Fonseca *et al.*, Refined mass and geometric measurements of the high-mass PSR J0740 + 6620, Astrophys. J. Lett. **915**, L12 (2021).
[12] B. P. Abbott *et al.*, Gravitational waves and gamma-rays from a binary neutron star merger: GW170817 and GRB 170817A, Astrophys. J. Lett. **848**, L13 (2017).
[13] B. P. Abbott *et al.* (LIGO Scientific Collaboration and Virgo Collaboration), Gw170817: Observation of gravitational waves from a binary neutron star inspiral, Phys. Rev. Lett. **119**, 161101 (2017).
[14] B. Abbott *et al.* (LIGO Scientific and Virgo Collaborations), GW170817: Measurements of neutron star radii and equation of state, Phys. Rev. Lett. **121**, 161101 (2018).
[15] B. Abbott *et al.* (LIGO Scientific and Virgo Collaborations), Properties of the binary neutron star merger GW170817, Phys. Rev. X **9**, 011001 (2019).
[16] M. Miller *et al.*, PSR J0030 + 0451 mass and radius from NICER data and implications for the properties of neutron star matter, Astrophys. J. Lett. **887**, L24 (2019).
[17] T. E. Riley *et al.*, A NICER view of PSR J0030 + 0451: Millisecond pulsar parameter estimation, Astrophys. J. Lett. **887**, L21 (2019).
[18] M. C. Miller *et al.*, The radius of PSR J0740 + 6620 from NICER and XMM-Newton data, Astrophys. J. Lett. **918**, L28 (2021).
[19] T. E. Riley *et al.*, A NICER view of the massive pulsar PSR J0740 + 6620 informed by radio timing and XMM-Newton spectroscopy, Astrophys. J. Lett. **918**, L27 (2021).

[20] K. Hebeler, J. M. Lattimer, C. J. Pethick, and A. Schwenk, Equation of state and neutron star properties constrained by nuclear physics and observation, Astrophys. J. **773**, 11 (2013).
[21] J. E. Lynn, I. Tews, J. Carlson, S. Gandolfi, A. Gezerlis, K. E. Schmidt, and A. Schwenk, Chiral three-nucleon interactions in light nuclei, neutron-α scattering, and neutron matter, Phys. Rev. Lett. **116**, 062501 (2016).
[22] J. Hu, Y. Zhang, E. Epelbaum, U.-G. Meißner, and J. Meng, Nuclear matter properties with nucleon-nucleon forces up to fifth order in the chiral expansion, Phys. Rev. C **96**, 034307 (2017).
[23] J. W. Holt and N. Kaiser, Equation of state of nuclear and neutron matter at third-order in perturbation theory from chiral effective field theory, Phys. Rev. C **95**, 034326 (2017).
[24] C. Drischler, R. J. Furnstahl, J. A. Melendez, and D. R. Phillips, How well do we know the neutron-matter equation of state at the densities inside neutron stars? A Bayesian approach with correlated uncertainties, Phys. Rev. Lett. **125**, 202702 (2020).
[25] C. Drischler, S. Han, J. M. Lattimer, M. Prakash, S. Reddy, and T. Zhao, Limiting masses and radii of neutron stars and their implications, Phys. Rev. C **103**, 045808 (2021).
[26] T. Gorda, A. Kurkela, P. Romatschke, M. Säppi, and A. Vuorinen, Next-to-next-to-next-to-leading order pressure of cold quark matter: Leading logarithm, Phys. Rev. Lett. **121**, 202701 (2018).
[27] G. Lugones, M. Mariani, and I. F. Ranea-Sandoval, A model-agnostic analysis of hybrid stars with reactive interfaces, J. Cosmol. Astropart. Phys. 03 (2023) 028.
[28] V. Sagun, E. Giangrandi, T. Dietrich, O. Ivanytskyi, R. Negreiros, and C. Providência, What is the nature of the HESS J1731-347 compact object?, Astrophys. J. **958**, 49 (2023).
[29] S. Kubis, W. Wójcik, D. A. Castillo, and N. Zabari, Relativistic mean-field model for the ultracompact low-mass neutron star HESS J1731-347, Phys. Rev. C **108**, 045803 (2023).
[30] P. Laskos-Patkos, P. S. Koliogiannis, and C. C. Moustakidis, Hybrid stars in light of the HESS J1731-347 remnant and the PREX-II experiment, Phys. Rev. D **109**, 063017 (2024).
[31] F. Di Clemente, A. Drago, and G. Pagliara, Is the compact object associated with HESS J1731-347 a strange quark star?, Astrophys. J. **967**, 159 (2024).
[32] J. E. Horvath, L. S. Rocha, L. M. de Sá, P. H. R. S. Moraes, L. G. Barão, M. G. B. de Avellar, A. Bernardo, and R. R. A. Bachega, A light strange star in the remnant hess J1731-347: Minimal consistency checks, Astron. Astrophys. **672**, L11 (2023).
[33] H. C. Das and L. L. Lopes, Anisotropic strange stars in the spotlight: Unveiling constraints through observational data, Mon. Not. R. Astron. Soc. **525**, 3571 (2023).
[34] G. Lugones and A. G. Grunfeld, Excluded volume effects in the quark-mass density-dependent model: Implications for the equation of state and compact star structure, Phys. Rev. D **109**, 063025 (2024).
[35] G. Lugones and A. G. Grunfeld, Strange quark stars: The role of excluded volume effects, Universe **10**, 233 (2024).
[36] J. P. Pereira, C. V. Flores, and G. Lugones, Phase transition effects on the dynamical stability of hybrid neutron stars, Astrophys. J. **860**, 12 (2018).
[37] M. Mariani, M. G. Orsaria, I. F. Ranea-Sandoval, and G. Lugones, Magnetized hybrid stars: Effects of slow and rapid phase transitions at the quark–hadron interface, Mon. Not. R. Astron. Soc. **489**, 4261 (2019).
[38] M. C. Rodríguez, I. F. Ranea-Sandoval, M. Mariani, M. G. Orsaria, G. Malfatti, and O. M. Guilera, Hybrid stars with sequential phase transitions: The emergence of the g2 mode, J. Cosmol. Astropart. Phys. 02 (2021) 009.
[39] D. Curin, I. F. Ranea-Sandoval, M. Mariani, M. G. Orsaria, and F. Weber, Hybrid stars with color superconducting cores in an extended fcm model, Universe **7**, 370 (2021).
[40] M. Mariani, L. Tonetto, M. C. Rodríguez, M. O. Celi, I. F. Ranea-Sandoval, M. G. Orsaria, and A. Pérez Martínez, Oscillating magnetized hybrid stars under the magnifying glass of multimessenger observations, Mon. Not. R. Astron. Soc. **512**, 517 (2022).
[41] V. P. Gonçalves and L. Lazzari, Impact of slow conversions on hybrid stars with sequential QCD phase transitions, Eur. Phys. J. C **82**, 288 (2022).
[42] I. F. Ranea-Sandoval, O. M. Guilera, M. Mariani, and G. Lugones, Breaking of universal relationships of axial w I modes in hybrid stars: Rapid and slow hadron-quark conversion scenarios, Phys. Rev. D **106**, 043025 (2022).
[43] I. F. Ranea-Sandoval, M. Mariani, G. Lugones, and O. M. Guilera, Constraining mass, radius, and tidal deformability of compact stars with axial wI modes: New universal relations including slow stable hybrid stars, Mon. Not. R. Astron. Soc. **519**, 3194 (2023).
[44] I. F. Ranea-Sandoval, M. Mariani, M. O. Celi, M. C. Rodríguez, and L. Tonetto, Asteroseismology using quadrupolar f -modes revisited: Breaking of universal relationships in the slow hadron-quark conversion scenario, Phys. Rev. D **107**, 123028 (2023).
[45] P. B. Rau and A. Sedrakian, Two first-order phase transitions in hybrid compact stars: Higher-order multiplet stars, reaction modes, and intermediate conversion speeds, Phys. Rev. D **107**, 103042 (2023).
[46] S. Ghosh, S. Ranjan Mohanty, T. Zhao, and B. Kumar, Exploring radial oscillations in slow stable and hybrid neutron stars, arXiv:2401.08347.
[47] I. A. Rather, K. D. Marquez, B. C. Backes, G. Panotopoulos, and I. Lopes, Radial oscillations of hybrid stars and neutron stars including delta baryons: The effect of a slow quark phase transition, J. Cosmol. Astropart. Phys. 05 (2024) 130.
[48] M. F. O'Boyle, C. Markakis, N. Stergioulas, and J. S. Read, Parametrized equation of state for neutron star matter with continuous sound speed, Phys. Rev. D **102**, 083027 (2020).
[49] G. Baym, C. Pethick, and P. Sutherland, The ground state of matter at high densities: Equation of state and stellar models, Astrophys. J. **170**, 299 (1971).
[50] G. Baym, H. A. Bethe, and C. J. Pethick, Neutron star matter, Nucl. Phys. A **175**, 225 (1971).
[51] A. Kurkela, P. Romatschke, and A. Vuorinen, Cold quark matter, Phys. Rev. D **81**, 105021 (2010).
[52] E. Annala, T. Gorda, A. Kurkela, J. Nättilä, and A. Vuorinen, Evidence for quark-matter cores in massive neutron stars, Nat. Phys. **16**, 907 (2020).

[53] M. Shibata, E. Zhou, K. Kiuchi, and S. Fujibayashi, Constraint on the maximum mass of neutron stars using GW170817 event, Phys. Rev. D **100**, 023015 (2019).
[54] L. Rezzolla, E. R. Most, and L. R. Weih, Using gravitational-wave observations and quasi-universal relations to constrain the maximum mass of neutron stars, Astrophys. J. Lett. **852**, L25 (2018).
[55] C. Musolino, C. Ecker, and L. Rezzolla, On the maximum mass and oblateness of rotating neutron stars with generic equations of state, Astrophys. J. **962**, 61 (2024).
[56] B. P. Abbott *et al.*, GW190425: Observation of a compact binary coalescence with total mass $\sim 3.4 M_{\odot}$, Astrophys. J. Lett. **892**, L3 (2020).
[57] M. G. Alford, G. Burgio, S. Han, G. Taranto, D. Zappalà, Constraining and applying a generic high-density equation of state, Phys. Rev. D **92**, 083002 (2015).
[58] G. Lugones and A. G. Grunfeld, Phase conversions in neutron stars: Implications for stellar stability and gravitational wave astrophysics, Universe **7**, 493 (2021).
[59] I. Bombaci, D. Logoteta, I. Vidana, and C. Providência, Quark matter nucleation in neutron stars and astrophysical implications, Eur. Phys. J. A **52**, 58 (2016).
[60] A. V. Olinto, On the conversion of neutron stars into strange stars, Phys. Lett. B **192**, 71 (1987).
[61] M. G. Alford, S. Han, and K. Schwenzer, Phase conversion dissipation in multicomponent compact stars, Phys. Rev. C **91**, 055804 (2015).
[62] G. Lugones and O. G. Benvenuto, Effect of trapped neutrinos in the hadron matter to quark matter transition, Phys. Rev. D **58**, 083001 (1998).
[63] G. Lugones, From quark drops to quark stars: Some aspects of the role of quark matter in compact stars, Eur. Phys. J. A **52**, 53 (2016).
[64] G. Malfatti, M. G. Orsaria, I. F. Ranea-Sandoval, G. A. Contrera, and F. Weber, Delta baryons and diquark formation in the cores of neutron stars, Phys. Rev. D **102**, 063008 (2020).
[65] P. B. Rau and G. G. Salaben, Nonequilibrium effects on stability of hybrid stars with first-order phase transitions, Phys. Rev. D **108**, 103035 (2023).
[66] B. Abbott *et al.* (LIGO Scientific and Virgo Collaborations), GW170817: Measurements of neutron star radii and equation of state, Phys. Rev. Lett. **121**, 161101 (2018).
[67] E. Lope Oter, A. Windisch, F. J. Llanes-Estrada, and M. Alford, nEoS: Neutron star equation of state from hadron physics alone, J. Phys. G Nucl. Phys. **46**, 084001 (2019).
[68] E. Lope-Oter and A. Wojnar, Constraining Palatini gravity with GR-independent equations of state for neutron stars, J. Cosmol. Astropart. Phys. 02 (2024) 017.
[69] A. Sorensen *et al.*, Dense nuclear matter equation of state from heavy-ion collisions, Prog. Part. Nucl. Phys. **134**, 104080 (2024).
[70] D. Blaschke, H. Grigorian, and D. Voskresensky, Cooling of hybrid neutron stars and hypothetical self-bound objects with superconducting quark cores, Astron. Astrophys. **368**, 561 (2001).
[71] J. Wei, G. Burgio, H. Schulze, and D. Zappalà, Cooling of hybrid neutron stars with microscopic equations of state, Mon. Not. R. Astron. Soc. **498**, 344 (2020).
[72] J. Zapata, T. Sales, P. Jaikumar, and R. Negreiros, Thermal relaxation and cooling of quark stars with a strangelet crust, Astron. Astrophys. **663**, A19 (2022).
[73] R. Catena and P. Ullio, A novel determination of the local dark matter density, J. Cosmol. Astropart. Phys. 08 (2010) 004.
[74] C. Kouvaris, WIMP annihilation and cooling of neutron stars, Phys. Rev. D **77**, 023006 (2008).